

Disks in Expanding FRW Universes

A. Feinstein, J. Ibáñez and Ruth Lazkoz

Dpto. Física Teórica, Universidad del País Vasco, E-48080 Bilbao, Spain;

wtpfexxa@lg.ehu.es, wtpibmej@lg.ehu.es and wtblasar@lg.ehu.es

ABSTRACT

We construct exact solutions to Einstein equations which represent relativistic disks immersed into an expanding FRW Universe. It is shown that expansion influences dynamical characteristics of the disks such as rotational curves, surface mass density, etc. The effects of the expansion is exemplified with non-static generalizations of Kuzmin-Curzon and generalized Schwarzschild disks.

Subject headings: celestial mechanics, stellar dynamics — cosmology: large scale structure of the Universe — galaxies: kinematics and dynamics — ISM: kinematics and dynamics — relativity

1. Introduction

Recently, there has been a renewed interest in the study of relativistic disks (Bičák, Lynden-Bell & Katz, 1993; Bičák & Ledvinka, 1993; & Bičák, Lynden-Bell & Pichon, 1993). The interest stems from a desire to address the possible observational evidence of giant black holes sustained by the surrounding disks.

The gravitational fields of galactic disks may be accurately modeled by the Newtonian potential theory of infinitesimally thin disks provided their thickness is negligible compared with the typical lengthscale of their halos. In more sound situations, however, when gravity is strong enough one must turn to General Relativity. A typical situation, where it is believed that Einstein theory may contribute firmly is met when accretion disks around the central black holes in quasars are considered. Disks can be also used to model sheet-like structures as well, so the study of relativistic disks may shed some light on the large scale inhomogeneities possibly present in the Universe (Lemos & Ventura 1994).

To consider disks in General Relativity, one usually starts with a static axially symmetric vacuum Weyl metric with a discontinuity in the first derivative across the azimuthal plane $z = 0$. The discontinuity in turn, induces distribution-like terms in the Ricci tensor. Everywhere outside the $z = 0$ plane the solution is vacuum with a non-vanishing surface mass density being the source of the geometry.

Since Weyl solutions are static in principle, these represent static disks which are not very interesting, for one would have serious trouble to explain the stability of such systems. To allow for rotation in General Relativity one must drop the assumption of the orthogonality of the two Killing vector fields associated with Weyl geometry. This may complicate the problem seriously introducing the dragging of an inertial reference frame.

Fortunately, Morgan and Morgan (1969a; 1969b; 1970) had the very smart idea of interpreting the “static disks” as to be made of two equal streams of collisionless particles circulating in opposite directions around a center. Interestingly enough, there exists observational evidence of some galaxies with two counterrotating stellar components around their center (Rix, Franx, Fisher & Illingworth 1992; Merrifield & Kuijken 1994; Bertola et al. 1996; Kuijken, Fisher & Merrifield 1996).

Another interpretational problem with so obtained solutions arises due to the fact that the disks are infinite in their extent in the azimuthal plane. It is believed, however, that any stellar or gas disk may be unstable to the so-called edge modes, should there be a sharp cut-off near the edges. One may also argue that infinite disks safely model the inner portions of galaxies or accretion disks.

Once the interpretational problems are dealt with, and given the linear character of the generating function of the Weyl metric, it is not difficult to start modeling relativistic disks in order to study their physical properties such as velocity profiles, surface mass density redshifts and so on.

Bičák, Lynden-Bell and Katz (1993, hereafter BLK) have used the result due to Evans and de Zeeuw (1992) enabling to analyze any classical axially symmetric disk into a linear superposition of so-called Kuzmin disks (Kuzmin 1956), together with the fact that the Weyl geometries may be generated by the solutions of the Laplace's equation, and constructed families of counterrotating disk space-times. This work was further extended by Bičák, Lynden-Bell (1993, hereafter BLP) and more recently by Lynden-Bell and Pichon (1996).

Lemos and Letelier (1993; 1994; 1996) using the well known techniques of superposing different Weyl solutions, have constructed space-times describing systems consisting of a Schwarzschild black hole surrounded by a disk.

The main purpose of this paper is to consider, in the framework of exact solutions in General Relativity, the effect of the cosmological expansion on the disk dynamics on one hand, and the influence of disk-like large-scale structures on the cosmological model kinematics on the other. For galactic and accretion disks fueling the quasars these effects are not expected to be spectacular, though the overall expansion may change the disk dynamics as will be seen later. For disk-like large-scale structures, however, the expansion is of particular importance.

In §2 we propose an algorithm to generate solutions to Einstein equations which may be interpreted as inhomogeneities imbedded in a spatially flat isotropic Universe. The technique uses a scalar field generalization of static Weyl solutions to the ones in a cosmological setting. The scalar field splits into two parts, one homogenous, which may be hydrodynamically interpreted as a velocity potential of an adiabatic perfect fluid, and another one highly irregular which may be thought of as a local disk inhomogeneity. The homogenous perfect fluid acts as a source of the FRW expansion away from the disk. In §3 we explain the way Kuzmin static disks are constructed and generalized in general relativity and the procedure of the previous section is applied. We then evaluate the energy-momentum tensor for any such disk and interpret it as an object in a FRW background. §4 is devoted to study the dynamics of the disks with the emphasis of the effects of the expansion on pertinent dynamical and kinematical quantities. We conclude the paper with the discussion and future prospects.

2. Exact non-static solutions with axial symmetry

2.1. Solution cosmologization procedure

In this Section we obtain non-static solutions to Einstein field equations representing compact objects in a cosmological setting. We start with Weyl's line element which can be written as:

$$ds^2 = -e^{2\nu(\rho,z)} dt^2 + e^{-2\nu(\rho,z)} \rho^2 d\phi^2 + e^{-2\nu(\rho,z)+2\zeta(\rho,z)} (d\rho^2 + dz^2). \quad (1)$$

Throughout the paper we use $G = c = 1$.

It is well-known that vacuum static axially symmetric fields in general relativity can be generated starting with a Newtonian potential (Weyl 1917; Levi-Civita 1919a; Levi-Civita 1919b). For the space-times obtained in this way the metric function ν in equation (1) may be taken to be any classical solution of the Laplace’s equation in cylindrical coordinates, and the other metric function ζ is obtained by a quadrature.

New non-static metrics may be generated in two stages. First, starting from a vacuum solution of the Einstein equations for a metric given by equation (1), we construct a new static solution with a minimally coupled massless scalar field ψ as a source. For these space-times the energy-momentum tensor takes the form:

$$T_{ab} = \psi_{,a} \psi_{,b} - \frac{1}{2} g_{ab} \psi_{,c} \psi^{,c}, \quad (2)$$

and the set of Einstein equations is

$$\nu_{zz} + \nu_{\rho\rho} + \rho^{-1} \nu_{\rho} = 0, \quad (3)$$

$$\zeta_{zz} + \zeta_{\rho\rho} - \rho^{-1} \zeta_{\rho} + 2 \nu_{\rho}^2 = -\psi_{\rho}^2, \quad (4)$$

$$\zeta_{zz} + \zeta_{\rho\rho} + \rho^{-1} \zeta_{\rho} + 2 \nu_z^2 = -\psi_z^2, \quad (5)$$

$$\rho^{-1} \zeta_z - 2 \nu_{\rho} \nu_z = -\psi_z \psi_{\rho}, \quad (6)$$

along with the Klein-Gordon equation

$$\psi_{zz} + \psi_{\rho\rho} + \rho^{-1} \psi_{\rho} = 0. \quad (7)$$

It is easy to see that if ν_o and ζ_o solve the vacuum Einstein equations a solution to equations (3-7) is given by

$$\nu = \nu_o + C \log \rho, \quad (8)$$

$$\zeta = B \zeta_o + E \nu_o + F \log \rho, \quad (9)$$

$$\psi = A \nu_o + D \log \rho, \quad (10)$$

where the constants are subject to the following constraints

$$2C + AD = E, \quad (11)$$

$$A^2 + 2 = 2B, \quad (12)$$

$$D^2 + 2C^2 = 2F. \quad (13)$$

For the purposes of this work we will discard the logarithmic terms by setting the constants C, F and D to zero, ensuring thus asymptotic flatness at spatial infinity in a static case.

Once the massless scalar field metric has been constructed, we transform it into a non-static solution with a self-interacting scalar field with an exponential potential. The algorithm is originally due to Fonarev (1995); see as well the generalization by Feinstein, Ibáñez & Lazkoz (1995). The new solution in a synchronous system of coordinates reads

$$ds^2 = -e^{2\nu(\rho,z)} dt^2 + R^2(t) e^{-2\nu(\rho,z)} \left(\rho^2 d\phi^2 + e^{2\zeta(\rho,z)} (d\rho^2 + dz^2) \right) \quad (14)$$

where the “scale factor” is $R(t) = t^{2/k^2}$ and the new metric functions are

$$\nu = \nu_o \quad \text{and} \quad \zeta = (1 + 2/k^2) \zeta_o, \quad (15)$$

with k being the slope of the potential $V = \Lambda e^{-k\psi}$. The line element in equation (14) is a solution of the Einstein field equations with the energy momentum tensor given by

$$T_{ab} = \psi_{,a}\psi_{,b} - g_{ab} \left(\frac{1}{2} \psi_{,i}\psi^{,i} + \Lambda e^{-k\psi} \right). \quad (16)$$

where $\Lambda = (12 - 2k^2)/k^4$.

The scalar field splits into a homogeneous part and an inhomogeneous one, $\psi(t, \rho, z) = \psi_h + \psi_{inh}$ with ψ_h and ψ_{inh} given by

$$\psi_h = \frac{2}{k} \log t \quad \text{and} \quad \psi_{inh} = \frac{2}{k} \nu_o. \quad (17)$$

Note that in the particular case $k^2 = 6$ the potential term vanishes, and one is left with a dynamical massless scalar field.

2.2. Interpretation of the new solutions

As long as the seed static metric is asymptotically flat, the newly generated non-static solution will become asymptotically homogeneous and isotropic. We stick to this kind of solutions, so at spatial infinity the geometry is represented by the FRW metric

$$ds^2 = -dt^2 + t^{4/k^2} (\rho^2 d\phi^2 + d\rho^2 + dz^2). \quad (18)$$

We now identify the homogeneous part of the scalar field with the velocity potential of a perfect fluid. The source of the expansion may be taken as an irrotational fluid with the energy-momentum tensor given by

$$T_{ab}^{FRW} = (p + \mu) u_a u_b + p g_{ab}. \quad (19)$$

The asymptotic four-velocity of the fluid is given by

$$u_a = \frac{\psi_{h,a} \delta_t^a}{\sqrt{(-\psi_{h,t} \psi^{h,t})}}, \quad (20)$$

so that the pressure p and the energy density μ become

$$\mu = -\frac{1}{2} \psi_{h,t} \psi^{h,t} + \Lambda t^{-2} \quad \text{and} \quad p = -\frac{1}{2} \psi_{h,t} \psi^{h,t} - \Lambda t^{-2}, \quad (21)$$

and substituting the scalar field we get

$$p = \frac{4k^2 - 12}{t^2 k^4} \quad \text{and} \quad \mu = \frac{12}{t^2 k^4}. \quad (22)$$

It is straightforward to see that the equation (22) defines the barotropic equation of state

$$p = \gamma \mu \quad \text{and} \quad \gamma = \frac{k^2 - 3}{3}. \quad (23)$$

Although the inhomogeneities steadily dilute as the spatial distance increases, they cannot be regarded to be negligible in the intermediate regions. The asymptotic homogeneity of the solution ensures that at any time the gradient of the scalar field is timelike only outside a certain closed spatial region, depending

basically on the mass and compactness of the disk, as well as on the strength of the scalar field. Outside this region the perfect fluid interpretation holds and the matter may be identified with the source of the overall expansion.

Another not unrelated question is the behaviour of the local disk-like inhomogeneities with time in the course of expansion. The character of the gradient of the scalar field serves us as a good indicator:

$$\psi_{,c}\psi^{,c} = \psi_{h,c}\psi^{h,c} + \psi_{inh,c}\psi^{inh,c} \quad (24)$$

where

$$\psi_{h,c}\psi^{h,c} = -\frac{4}{3\gamma+3}t^{-2}e^{-2\nu} \quad (25)$$

and

$$\psi_{inh,c}\psi^{inh,c} = \frac{4}{3\gamma+3}t^{-\frac{4}{3\gamma+3}}e^{2\nu-2\zeta}(\nu_{,r}^2 + \nu_{,z}^2). \quad (26)$$

We have checked that for the models with accelerated expansion $\gamma < -1/3$ the kinetic (homogeneous) term of the scalar field dominates that one representing the spatial gradients (inhomogeneities) and eventually the region where the gradient has a spatial character shrinks to zero, a fact which is consistent with the accelerated inflationary behaviour. For $\gamma > -1/3$ the region of inhomogeneity grows.

At sufficiently late times a certain hypersurface can be found such that constitutes a border between the region where the perfect-fluid interpretation is untenable, and another one occupied by an inhomogeneous cosmological fluid can be found. In the outside region the four velocity of the fluid reads

$$u_a = \frac{\psi_a}{\sqrt{(-\psi_{,c}\psi^{,c})}} \quad (27)$$

and the energy density and pressure have the following expressions:

$$\mu = -\frac{1}{2}\psi_{,c}\psi^{,c} + \Lambda e^{-k\psi} \quad \text{and} \quad p = -\frac{1}{2}\psi_{,c}\psi^{,c} - \Lambda e^{-k\psi}. \quad (28)$$

We could say that the highly inhomogeneous region surrounding the disk plane in which the perfect fluid interpretation is not valid plays the role of a cushion between the disk and the cosmological fluid, representing a transition region between both regimes.

One may interpret solutions of the type given in equation (14) as an inhomogeneity embedded in an expanding Universe on the grounds that on large scales one recovers the Friedmannian behaviour while the local structure for small distances is governed by the seed metric. This interpretation will be re-enforced in the light of the results of following sections.

3. Relativistic expanding Kuzmin disks

We now apply the described “cosmologization” algorithm to the well-known family of axially symmetric solutions representing infinitesimally thin disks in a relativistic context and construct their dynamical counterparts. We are mostly interested in the influence of expansion on the dynamical quantities that characterize the disks. It is expected that for an expanding Universe the mass-energy density on the disk plane will steadily decrease as time goes by. However, the effect on other magnitudes such as velocity or angular momentum is not intuitively foreseeable. In addition, we believe that the conclusions reached in this work for the particular matter distributions studied here can bring a new perspective onto the problem of embedding highly inhomogeneous sources into standard cosmologies.

3.1. Generation of Kuzmin disk families

The disk configurations we are dealing with were firstly studied by Morgan & Morgan (1969a, 1969b, 1970) and describe counterrotating disks with the same number of leftwise and rightwise rotating particles. This way of looking at the problem, apart from preventing the dragging of inertial frames, ensures stability of the solutions. It also allows the general relativistic description of those configurations by means of a Weyl’s metric, as well as the subsequent generalization to a cosmological setup by the method mentioned above.

As we pointed out in the previous section one can start with the Newtonian potential produced by a disk to obtain its relativistic version. We generically call any disk-like axially symmetric vacuum solution with a discontinuity across the $z = 0$ plane a Kuzmin disk (Kuzmin 1956). Recently these “static” disks were generalized by Pichon and Lynden-Bell (1996) to include true rotation and radial pressure. The new solutions were referred to as warm disks.

For the sake of simplicity, unless otherwise stated, we focus on two simple families of disks, the Kuzmin-Curzon disks and the generalized Schwarzschild disks which are built by superposing the potentials of simple Kuzmin-Curzon disks. Although relatively simple, the Kuzmin-Curzon disks model very interesting physical configurations. Remarkably as well, they may be used as building blocks of more complicated disk-like solutions; one should just superpose elementary Kuzmin-Curzon disks with different compactities weighted by a function $W(b)$, as shown by Evans & de Zeeuw (1992). Their work on Newtonian axisymmetric potential-density pairs was extended to a relativistic case by BLK, who gave the general form of the metric for a superposition of Kuzmin-Curzon disks.

BLP gave a step further in the study of relativistic disks by constructing the more involved families of relativistic versions of the Kuzmin-Toomre (Toomre 1963; Nagai & Miyamoto 1976; Evans & de Zeeuw 1992) and Kalnajs-Mestel disks (Mestel 1963; Kalnajs 1976). The latter family of solutions is specially remarkable because they have long and flat rotation curves for certain values of the parameters. The lowest order representatives of that set of disks are the so-called generalized Schwarzschild disks and we are choosing them to illustrate our algorithm, together with Kuzmin-Curzon disks for they are quite simple but as interesting as any of the members of the Kalnajs-Mestel family .

The potential corresponding to Kuzmin-Curzon disks is obtained by introducing a discontinuity in the original Curzon metric (Curzon 1924; Chazy 1924) using the transformation $z \rightarrow |z| + b$. This way of introducing the discontinuity is equivalent to placing on the z axis two mirror particles of mass M at a distance b below and above the $z = 0$ plane in a classical picture. The Newtonian potential for the Kuzmin-Curzon disk is

$$\nu_o^{K-C} = -\frac{M}{[\rho^2 + (|z| + b)^2]^{\frac{1}{2}}} \quad (29)$$

and following Weyl, one identifies it with the metric function ν_o in equation (10). The metric function ν_o remains a solution of the Laplace’s equation outside the $z = 0$ plane, but now due to the discontinuity, there appears to be a non-vanishing surface mass density. Integration of the remaining metric function yields

$$\zeta_o^{K-C} = -\frac{M^2 \rho^2}{[\rho^2 + (|z| + b)^2]^2}. \quad (30)$$

Correspondingly, as shown by BLK the classical surface mass density $\Sigma(\rho) = 2 \nu_{o,z}|_{z=0+}$ is

$$\Sigma^{K-C} = \frac{4 M b}{(\rho^2 + b^2)^{\frac{3}{2}}}. \quad (31)$$

Here M is the total mass of the disk as measured from the infinity, and b is a parameter measuring the compactness of the disk.

The analogue of a generalized Schwarzschild disk is constructed in the classical Kuzmin's picture by substituting the two mirror particles by two rods with constant line density. Then, the general relativistic solution is given by

$$\nu_o^{G-S} = \frac{M}{b_{max} - b_{min}} \log \left| \frac{\rho_{min} + |z| + b_{min}}{\rho_{max} + |z| + b_{max}} \right| \quad (32)$$

and

$$\zeta_o^{G-S} = \frac{2 M^2}{(b_{max} - b_{min})^2} \log \left| \frac{(\rho_{min} + \rho_{max})^2 - (b_{max} - b_{min})^2}{4 \rho_{min} \rho_{max}} \right|. \quad (33)$$

In this case, the classical surface mass density $\Sigma(\rho)$ is

$$\Sigma^{G-S} = \frac{4 M}{(b_{max} - b_{min}) (\rho^2 + b^2)^{\frac{1}{2}}} \Big|_{b_{max}}^{b_{min}}, \quad (34)$$

where $\rho_{min}^2 = \rho^2 + (|z| + b_{min})^2$ and $\rho_{max}^2 = \rho^2 + (|z| + b_{min})^2$, being $b_{max} - b_{min}$ the parameter that measures the compactness of the disk.

3.2. Disks expanding in a FRW Universe

We start by looking somewhat more carefully at the stress-energy tensor for the obtained solutions given by equation (14) with the metric functions corresponding to a generic thin counterrotating disk.

In order to deal with the discontinuities in the metric across the $z = 0$ plane, we consider the metric functions in the sense of distributions and introduce a new variable $\xi = |z|$. Generically the metric coefficients will have square-integrable weak derivatives, and so the usual formula for the Ricci tensor can be interpreted in the sense of distributions. The stress-energy tensor reads (cf. as well Chamorro, Gregory & Stewart, 1987)

$$T_\rho^\rho - T_z^z = 2 R(t)^{-2} (\rho^{-1} \zeta_{,\rho} + \nu_{,\xi}^2 - \nu_{,\rho}^2) e^{-2\zeta+2\nu} \quad (35)$$

$$T_\rho^\rho + T_z^z = -2 R(t)^{-2} (\dot{R}^2 + 2R\ddot{R}) e^{-2\nu} \quad (36)$$

$$\begin{aligned} T_t^t + T_\phi^\phi &= -2 R(t)^{-2} (\nu_{,\rho\rho} + \nu_{,\xi\xi} + 2\delta(z)\nu_{,\xi} + \rho^{-1}\nu_{,\rho} - \zeta_{,\rho\rho} - \zeta_{,\xi\xi} \\ &\quad - 2\delta(z)\zeta_{,\xi} - \nu_{,\rho}^2 - \nu_{,\xi}^2) e^{-2\zeta+2\nu} \\ &\quad - 2 R(t)^{-2} (2\dot{R}^2 + R\ddot{R}) e^{-2\nu} \end{aligned} \quad (37)$$

$$\begin{aligned} T_t^t - T_\phi^\phi &= -2 R(t)^{-2} (\nu_{,\rho\rho} + \nu_{,\xi\xi} + 2\delta(z)\nu_{,\xi} + \rho^{-1}\nu_{,\rho}) e^{-2\zeta+2\nu} \\ &\quad - 2 R(t)^{-2} (\dot{R}^2 - R\ddot{R}) e^{-2\nu} \end{aligned} \quad (38)$$

$$T_z^z = -2 R(t)^{-2} [\theta(z) - \theta(-z)] (2\nu_{,\rho}\nu_{,\xi} - \rho^{-1}\zeta_{,\xi}) e^{-2\zeta+2\nu} \quad (39)$$

$$T_t^\rho = 2 R(t)^{-3} \dot{R} \nu_{,\rho} e^{-2\zeta+2\nu} \quad (40)$$

$$T_t^z = 2 R(t)^{-3} [\theta(z) - \theta(-z)] \dot{R} \nu_{,\xi} e^{-2\zeta+2\nu} \quad (41)$$

The energy-momentum tensor given by equations (35-41) splits into a regular part and a singular one proportional to the functional $\delta(z)$, which is interpreted as a thin counterrotating disk. We still separate

the regular part into two bits: a highly inhomogeneous part vanishing at infinity that we interpret as an interaction term between the matter composing the disk and that of the cosmic fluid, and another part behaving at infinity as that of an isotropic perfect fluid which we attribute to a global expansion. Phenomenologically we write

$$T_a^b = T_a^{b\,disk} + T_a^{b\,int} + e^{-2\nu} T_a^{b\,FRW}. \quad (42)$$

where

$$T_t^{t\,FRW} = 3 R(t)^{-2} \dot{R}^2 \quad (43)$$

and

$$T_\phi^{\phi\,FRW} = T_\rho^{\rho\,FRW} = T_z^{z\,FRW} = -2 R(t)^{-2} (\dot{R}^2 + 2 R \ddot{R}). \quad (44)$$

The identification of the other terms is straightforward. The term we have referred to as $T_a^{b\,disk}$ is precisely the one which is discontinuous across the $z = 0$ plane and which therefore gives rise to the non vanishing mass density. One has to be careful when interpreting equation (42), for it has a purely phenomenological character. Obviously none of the three terms in the r.h.s. of equation (42) can be regarded as a true energy-momentum tensor, since they do not satisfy the energy conservation equation $T_{;b}^{a,b} = 0$ separately. Note, that this decomposition into three terms is similar to that proposed in §2.2 based on the character of the gradient of the scalar field. Both approaches qualitatively lead to the same physical description.

4. Dynamics of expanding disks

In this Section we study the dynamical magnitudes of relativistic disks and discuss the influence of expansion on those. We explicitly prove that the mass-energy density decreases with time due to the expansion, and also address the question of the effect of the expansion on the flattening of the rotation curves.

Special attention will be paid to the comparison between a static disk and its counterpart in a pressure-free Universe. Our motivation is that the Universe, as observed at present, has negligible pressure up to local inhomogeneities.

We now look at the surface mass density and streaming velocities of the particles on the disk. The τ_a^b surface components are obtained by integration across the disk of the T_a^b components of the energy-momentum tensor,

$$\tau_a^b = \int T_a^b R(t) e^{(\zeta-\nu)} dz. \quad (45)$$

As shown by BLK, the surface rest mass density in a fixed reference system reads $\sigma_0 = 2\sigma_p(1-v^2)^{-1/2}$, while the surface mass density in the same reference system is $\sigma = 2\sigma_p(1-v^2)^{-1} = \sigma_p(1-v^2)^{-1/2}$, being v the rotational velocity and σ_p the proper rest mass density of one stream.

Firstly, one may calculate the surface mass density $\sigma(\rho, t)$ on the disk plane by integrating the T_t^t term across the disk. Using equations (37,38) one gets

$$\sigma(\rho, t) = -\tau_t^t = -\int_{0-}^{0+} T_t^t R(t) e^{(\zeta-\nu)} dz = R(t)^{-1} e^{(\nu-\zeta)} (4\nu_{,\xi} - 2\zeta_{,\xi})|_{\xi=0}, \quad (46)$$

and substituting $\zeta_{,\xi}$ calculated from the equation (6) we obtain after some algebra

$$\sigma(\rho, t) = 4 R(t)^{-1} \nu_{,\xi} e^{(\nu-\zeta)} (1 - \rho f(\gamma) \nu_{,\rho})|_{\xi=0}, \quad (47)$$

where we denote $f(\gamma) = (3\gamma + 3)/(3\gamma + 5)$ and just remind that γ is the adiabatic index of the perfect fluid.

Note that the static case will be recovered in the limit $\gamma \rightarrow \infty$, $f(\gamma) \rightarrow 1$. The particular case of a dust filled Universe corresponds to $\gamma = 0$ and $f(\gamma) = 3/5$.

By integrating the T_ϕ^ϕ term obtained from equations (37,38) one gets

$$v^2 \sigma = \tau_\phi^\phi = \int_{0-}^{0+} T_\phi^\phi R(t) e^{(\zeta-\nu)} dz = 2 R(t)^{-1} e^{(\nu-\zeta)} f(\gamma) \zeta, \xi|_{\xi=0} \quad (48)$$

or alternatively

$$v^2 \sigma = 4 R(t)^{-1} e^{(\nu-\zeta)} \rho f(\gamma) \nu, \rho \nu, \xi|_{\xi=0} \quad (49)$$

Then, from equations (47,49) one readily obtains the streaming velocities

$$v^2 = \frac{\rho f(\gamma) \nu, \rho}{1 - \rho f(\gamma) \nu, \rho} \Big|_{\xi=0}. \quad (50)$$

To emphasize the difference in the flattening of the rotation curves in the static and expanding cases we also evaluate the derivative of the velocity in the radial direction obtaining

$$v_\rho = - \frac{f(\gamma)^{1/2} \nu, \xi \xi}{2 [\nu, \rho (1 - \rho f(\gamma) \nu, \rho)]^{1/2}} \Big|_{\xi=0}. \quad (51)$$

Since the classical mass density $\Sigma(r) = 4 \nu, \xi|_{\xi=0}$ of the disks under consideration is positive everywhere, to ensure the positivity of the surface energy density σ we must impose $r f(\gamma) \nu, r|_{\xi=0} < 1$, as it can be deduced from equation (47). This is equivalent to the fulfillment of the weak energy condition (cf. BLK). For the particular case of an expanding Kuzmin-Curzon disk this restriction reduces to

$$\frac{M f(\gamma)}{b} < \frac{\sqrt{27}}{2}, \quad (52)$$

whereas for a generalized Schwarzschild disk it becomes

$$\frac{M}{(b_{max} - b_{min})} < \frac{[1 - (b_{min}/b_{max})^2]^{\frac{1}{2}}}{[1 - (b_{min}/b_{max})^{\frac{2}{3}}]^{\frac{3}{2}}}. \quad (53)$$

Moreover, if $\rho f(\gamma) \nu, \rho|_{\xi=0} < 1/2$ the dominant energy-condition holds and the rotation velocities are lower than that of light. It is clear that as long as the dominant energy condition holds the positivity of the mass density is also ensured. That restriction for Kuzmin-Curzon disks reads

$$\frac{M f(\gamma)}{b} < \frac{\sqrt{27}}{4}, \quad (54)$$

and for generalized Schwarzschild disks it becomes

$$\frac{2 M}{(b_{max} - b_{min})} < \frac{[1 - (b_{min}/b_{max})^2]^{\frac{1}{2}}}{[1 - (b_{min}/b_{max})^{\frac{2}{3}}]^{\frac{3}{2}}}. \quad (55)$$

To compare the streaming velocities of a static disk and any of its time-evolving counterparts, one may look now at the expression of their quotient, which reads

$$\frac{v^2(\gamma)}{v^2(\gamma = \infty)} = f(\gamma) \frac{1 - \rho \nu, \rho}{1 - \rho f(\gamma) \nu, \rho} \Big|_{\xi=0}. \quad (56)$$

Since in every case $f(\gamma) \leq 1$, we conclude that typically for expanding disks the velocities are everywhere lower than those for a static one (see Figure 1).

To compare the results with those obtained by BLK we show in the plots the dynamical magnitudes as functions of the *circumferential* radius $\rho_c = \rho e^{-\nu}$, being $2\pi\rho_c$ the physical circumference of a $\rho = \text{constant}$ circle. Note, that for the solutions studied in this paper the comoving radius does not depend on the γ parameter.

Yet, more interesting conclusions are obtained from the quotient between the velocity derivatives in the radial direction,

$$\frac{v_{,\rho}(\gamma)}{v_{,\rho}(\gamma = \infty)} = f^{1/2}(\gamma) \left(\frac{1 - \rho \nu_{,\rho}}{1 - \rho f(\gamma) \nu_{,\rho}} \right)^{3/2} \Big|_{\xi=0}. \quad (57)$$

From equation (57) it can be learnt that the slope of the rotation curves for expanding disks is less pronounced than for static ones. Thus, the conclusion is reached that the expansion makes the flattening of the rotation curves more sound (see Figure 2).

Another question to dwell on is how the mass-energy density on the disk plane changes with the introduction of time dependence. Similarly to the procedure used above for velocities we look at the quotient of the magnitudes for a disk with an arbitrary value of γ and a static disk,

$$\frac{\sigma(\gamma)}{\sigma(\gamma = \infty)} = \frac{1 - \rho f(\gamma) \nu_{,\rho}}{1 - \rho \nu_{,\rho}} (t e^{\zeta_0})^{-\frac{2}{3\gamma+3}} \quad (58)$$

Since in the cases under consideration ζ_0 is a negative function everywhere on the disk, it can be concluded that expanding disks are denser than static ones, with their additional mass concentrated outside the center, whereas the central value is not affected by the expansion. Time-evolution of this magnitude crucially depends on the adiabatic index γ . To be more specific, the mass-density dilution rate increases, keeps constant or decreases with time, if the expansion parameter γ is less, equal or bigger than $-1/3$ respectively.

It is also interesting to examine the surface rest mass density of the rotating particles as measured in a frame attached to fixed axes. This quantity is given by

$$\sigma_0 = \sigma (1 - v^2)^{1/2}. \quad (59)$$

Substituting the expression for σ and v in equations (47,50) we get

$$\sigma_0(\rho, t) = 4 \nu_{,\xi} e^{(\nu-\zeta)} [1 - \rho f(\gamma) \nu_{,\rho}]^{\frac{1}{2}} [1 - 2 \rho f(\gamma) \nu_{,\rho}]^{\frac{1}{2}} \Big|_{\xi=0} \quad (60)$$

The latter quantity is everywhere positive provided the dominant energy condition holds. Taking the previous results into account, it is straightforward to see that the behaviour of surface rest mass density σ_0 with time and with respect to the index γ is the same as for the mass density σ .

We have defined two new functions $\Delta\sigma/\sigma$ and $\Delta\sigma_0/\sigma_0$ which give the contrast in surface mass density and surface rest mass density respectively between an expanding disk and a static one. Figures 3a and 3b represent the contrast function $\Delta\sigma/\sigma$ and Figures 4a and 4b give their rest counterparts $\Delta\sigma_0/\sigma_0$ for both a generalized Schwarzschild disk and a Kuzmin-Curzon disk. It can be seen from the figures that the expanding disks having the same mass parameter M are much denser than their static counterparts.

Finally, it is worth looking at the specific angular momentum of the counterrotating components of the disk. Bearing in mind that the specific angular momentum of a particle with rest mass m rotating at radius r is defined as

$$j = (p_{\phi\phi}/m) = g_{\phi\phi} d\phi/d\lambda, \quad (61)$$

where λ is proper time, then

$$j(\rho, t) = R(t) \frac{\rho v e^{-\nu}}{(1 - v^2)^{\frac{1}{2}}} \Big|_{\xi=0}, \quad (62)$$

or alternatively

$$j(\rho, t) = R(t) \frac{(\rho^3 f(\gamma) \nu_{,\rho})^{\frac{1}{2}} e^{-\nu}}{(1 - 2 \rho f(\gamma) \nu_{,\rho})^{\frac{1}{2}}} \Big|_{\xi=0}. \quad (63)$$

As it happened to the rotation velocities, a lower γ gives as well a lower angular momentum, which increases with time.

The results are presented in figures 5a and 5b where we compare the specific angular momentum in the pressure free and static Universes for a generalized Schwarzschild disk and a Kuzmin-Curzon disk.

5. Conclusions and outlook

We have constructed exact solutions to Einstein equations which we interpret as representing relativistic disks in a cosmological setting. A self interacting scalar field serves as the source of the global expansion on one hand, yet locally it defines a disk-like structure across the $z = 0$ plane. Far away from this plane the spatial gradients of the scalar field may be identified with the velocity potential of the irrotational perfect fluid with an adiabatic equation of state $p = \gamma\rho$. Near the azimuthal plane the spatial gradients of the scalar field dominate over the kinetic part and the geometry is highly inhomogeneous. No sharp-cut transition region exists in between these two different regimes, however, this probably corresponds to a physically more realistic situation than a surface matching between different solutions of gravitational field equations. Moreover, to the best of our knowledge, there do not exist such matched solutions in the case of axial symmetry and the external FRW geometry.

Some particular cases of the solutions we have considered ($k^2 = 6$) may be re-interpreted as disks in the Brans-Dicke theory. Indeed, in this case the scalar field may be considered as massless (the potential term vanishes) and a simple conformal transformation $ds^2 \rightarrow e^{\psi/\sqrt{\omega+3/2}} ds^2$ transforms the solution into a Brans-Dicke frame (Tabensky and Taub 1973).

The physical interpretation of the solutions then is quite different, these represent relativistic disks in a theory where the gravitational constant varies in space and time. We will not dwell more about this point here, but just mention that the analysis of our paper applies equally well to Brans-Dicke disks.

Once the solutions are interpreted as local inhomogeneities in a model Universe the way is cleared to see the effects produced by expansion. We have found that depending on the rate of expansion the inhomogeneities occupy larger or smaller regions of the Universe. More specifically, for the accelerated expansion we find that the inhomogeneities disappear with time, while in a decelerated model their growth is unlimited.

The effect of the expansion on the dynamical characteristics of the disks was studied as well. We have shown that expansion changes in principle the fall-off of the rotational curves, the angular momentum and

the surface mass density of the disks and have compared the characteristics of the static disks with those in a dust filled Universe.

Although we have concentrated our study on disk-like objects, it is remarkable that the generating technique we used to obtain solutions is also adequate to study other type of sources of astrophysical interest such as cosmic strings, walls, spherical shells, etc.

6. Acknowledgements

We are grateful to Wyn Evans, Sasha Kashlinsky, Konrad Kuijken and M. A. Vázquez-Mozo for correspondence and valuable suggestions. This work was partially supported by a Spanish Ministry of Education Grant (CICyT) PB93-0507 and a Basque Country University Grant UPV/EHU/72.310EBO36/95. R.L. acknowledges financial support from the Basque Government under Fellowship BFI94-094.

REFERENCES

- Bertola, F., Cinzano, P., Corsini, E.M., Pizzella, A., Persic, M., & Salucci, P. 1996, ApJ, 458, L67
- Bičák, J., Ledvinka, T. 1993, Phys. Rev. Lett. 71, 1669
- Bičák, J., Lynden-Bell, D., & Katz, J. 1993, Phys. Rev. D 47, 4334
- Bičák, J., Lynden-Bell, D., & Pichon, C. 1993, MNRAS, 265, 126
- Curzon, H. E. J. 1924, Proc. London Math. Soc. 23, 477
- Chamorro, A., Gregory, R., & Stewewart, J. M. 1987, Proc. R. Soc. London A, 413, 251
- Chazy, J. 1924, Bull. Soc. Math. Paris 52, 17
- Evans, N. W., & de Zeeuw, P. T. 1992, MNRAS, 257, 152
- Feinstein, A., Ibáñez, J., & Lazkoz, R. 1995, Class. Quantum. Grav., 12, L57
- Fonarev, O. A. 1995, Class. Quantum. Grav., 12, 1739
- Kalnajs, A., 1976, ApJ, 205, 751
- Kuijken, K., Fisher D., & Merrifield, M. R.. 1996, MNRAS, 283, 543
- Kuzmin, G. G. 1956, Astron. Zh., 33, 27
- Lemos, J. P. S., & Ventura, O. S. 1994, J. Math. Phys., 35, 3604
- Lemos J. P. S., & Letelier, P. S. 1993, Class. Quantum Grav., 10, L75
- Lemos J. P. S., & Letelier, P. S. 1994, Phys. Rev. D, 49, 5135
- Lemos J. P. S., & Letelier, P. S. 1996, Int. J. Mod. Phys. D, 5, 53
- Levi-Civita, T. 1919a, Rend. Acad. Lincei, 28, 3

- Levi-Civita, T. 1919b, *Rend. Acad. Lincei*, 28, 101
- Lynden-Bell, D., & Pichon, C. 1996, *MNRAS*, 280, 1007
- Merrifield, M.R., & Kuijken, K. 1994, *ApJ*, 432, 575
- Mestel L. 1963, *MNRAS*, 126, 553
- Morgan, T., & Morgan, L. 1969a, *Phys. Rev.*, 183, 1097
- Morgan, T., & Morgan, L. 1969b, *Phys. Rev.*, 188, 2544 (E)
- Morgan, T., & Morgan, L. 1970, *Phys. Rev. D*, 2, 2576
- Nagai, R., & Miyamoto, M. 1976, *PASJ*, 28, 1
- Rix, H., Fisher, H., & Illingworth, D. 1992, *ApJ*, 400, L5
- Tabensky, R., & Taub, A.H. 1973, *Commun. Math. Phys.* 29, 61
- Toomre, A., 1963, *ApJ*, 138, 385
- Weyl, H. 1917, *Ann. Phys. (N.Y.)*, 54, 307

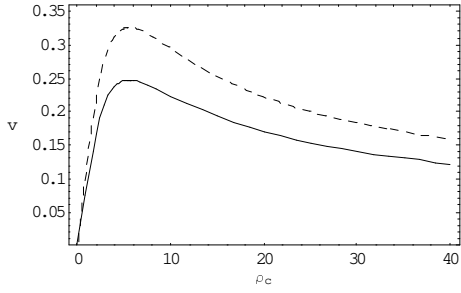


Fig. 1a

Fig. 1b

Fig. 1.— Streaming velocity v as function of the circumferential radius ρ_c for a generalized Schwarzschild disk with $M = 100$, $b_{min} = 1$ and $b_{max} = 200$ (a); and for a Kuzmin-Curzon disk with $M = 1$ and $b = 4$ (b). The continuous lines correspond to expanding disks in a dust filled FRW Universe, whereas the dashed lines correspond to their static counterparts.

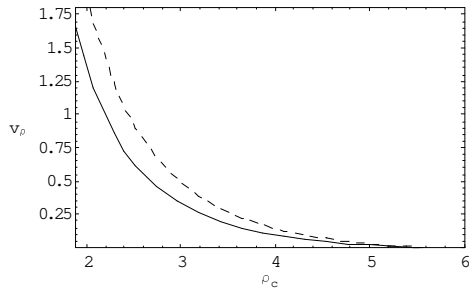


Fig. 2a

Fig. 2b

Fig. 2.— Radial derivative of the streaming velocity v_ρ as function of the circumferential radius ρ_c for a generalized Schwarzschild disk with $M = 100$, $b_{min} = 1$ and $b_{max} = 200$ (a); and a Kuzmin-Curzon disk with $M = 1$ and $b = 4$ (b). The continuous lines corresponds to expanding disks in a dust filled FRW Universe, whereas the dashed lines correspond to their static counterparts.

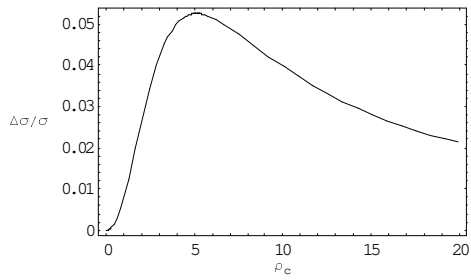


Fig. 3a

Fig. 3b

Fig. 3.— Surface energy density contrast $\Delta\sigma/\sigma$ at $t = 1$ as function of the circumferential radius ρ_c for a generalized Schwarzschild disk with $M = 100$, $b_{min} = 1$ and $b_{max} = 200$ (a); and for Kuzmin-Curzon disk with $M = 1$ and $b = 4$ (b).

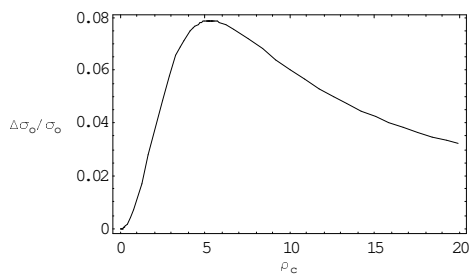


Fig. 4a

Fig. 4b

Fig. 4.— Surface rest energy density contrast $\Delta\sigma_0/\sigma_0$ at $t = 1$ as function of the circumferential radius ρ_c for a generalized Schwarzschild disk with $M = 100$, $b_{min} = 1$ and $b_{max} = 200$ (a); and a Kuzmin-Curzon disk with $M = 1$ and $b = 4$ (b).

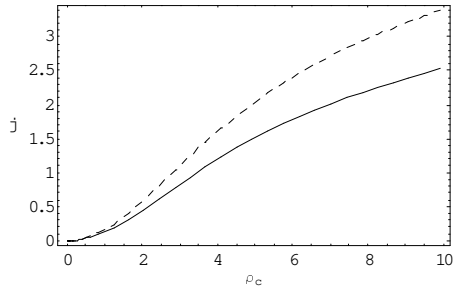


Fig. 5a

Fig. 5b

Fig. 5.— Specific angular momentum j at $t = 1$ as function of the circumferential radius ρ_c for a generalized Schwarzschild disk with $M = 100$, $b_{min} = 1$ and $b_{max} = 200$ (a); and for a Kuzmin-Curzon disk with $M = 1$ and $b = 4$ (b). The continuous lines correspond to disks in a dust filled FRW Universe, whereas the dashed lines correspond to their static counterparts.